nature structural & molecular biology

SUPPLEMENTARY INFORMATION

https://doi.org/10.1038/s41594-019-0305-z

In the format provided by the authors and unedited.

Cryo-EM structure and dynamics of eukaryotic DNA polymerase δ holoenzyme

Rinku Jain[1]*, William J. Rice[2], Radhika Malik[1], Robert E. Johnson[3], Louise Prakash[3], Satya Prakash[3], Iban Ubarretxena-Belandia[1,4,5] and Aneel K. Aggarwal[1]*

[1]Department of Pharmacological Sciences, Icahn School of Medicine at Mount Sinai, New York, NY, USA. [2]Simons Electron Microscopy Center, New York Structural Biology Center, New York, NY, USA. [3]Department of Biochemistry and Molecular Biology, University of Texas Medical Branch, Galveston, TX, USA. [4]Instituto Biofisika (UPV/EHU, CSIC), University of the Basque Country, Leioa, Spain. [5]Ikerbasque, Basque Foundation for Science, Bilbao, Spain. *e-mail: rinku.jain@mssm.edu; aneel.aggarwal@mssm.edu

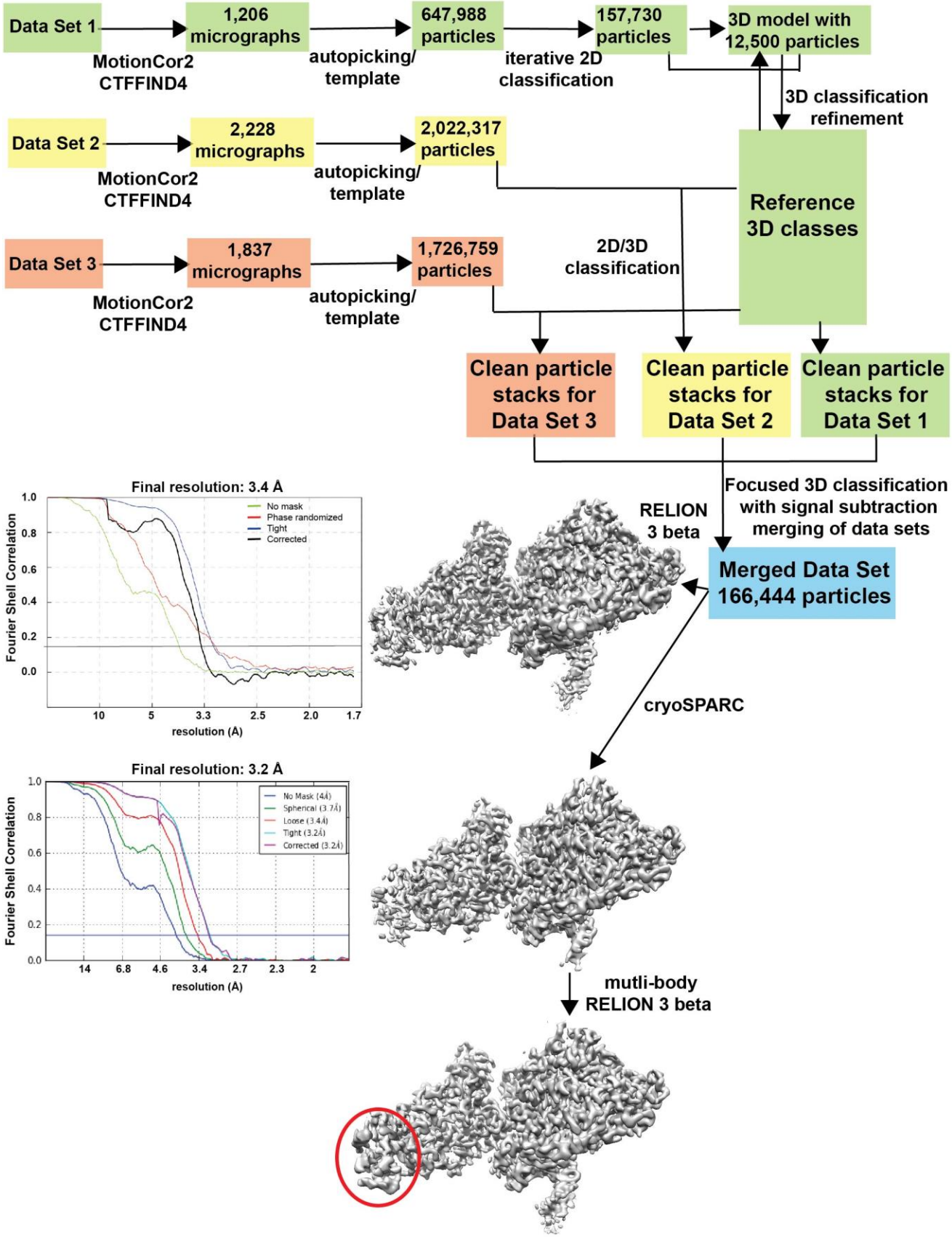
Data Set 1
1,206 micrographs
MotionCor2
CTFFIND4
647,988 particles
autopicking/ template
157,730 particles
iterative 2D classification
3D model with 12,500 particles
3D classification refinement
Data Set 2
2,228 micrographs
MotionCor2
CTFFIND4
2,022,317 particles
autopicking/ template
Reference 3D classes
Data Set 3
1,837 micrographs
MotionCor2
CTFFIND4
1,726,759 particles
autopicking/ template
2D/3D classification
Clean particle stacks for Data Set 3
Clean particle stacks for Data Set 2
Clean particle stacks for Data Set 1
Focused 3D classification with signal subtraction merging of data sets
Merged Data Set 166,444 particles
RELION 3 beta
cryoSPARC
mutli-body RELION 3 beta
Final resolution: 3.4 Å
Fourier Shell Correlation
resolution (Å)
No mask
Phase randomized
Tight
Corrected
Final resolution: 3.2 Å
No Mask (4Å)
Spherical (3.7Å)
Loose (3.4Å)
Tight (3.2Å)
Corrected (3.2Å)

Supplementary Figure 1

Cryo-EM structure of DNA bound Polδ holoenzyme.

Particles from three different data sets were merged and 3D refinement was performed with both cryoSPARC and RELION 3.0 beta to yield consensus maps at nominal resolution of 3.2 and 3.4 Å respectively. Consensus map from RELION was subjected to multi-body refinement, resulting in major improvement in density for Pol32N (circled in red) and regions of Pol31 that are furthest from the catalytic module.

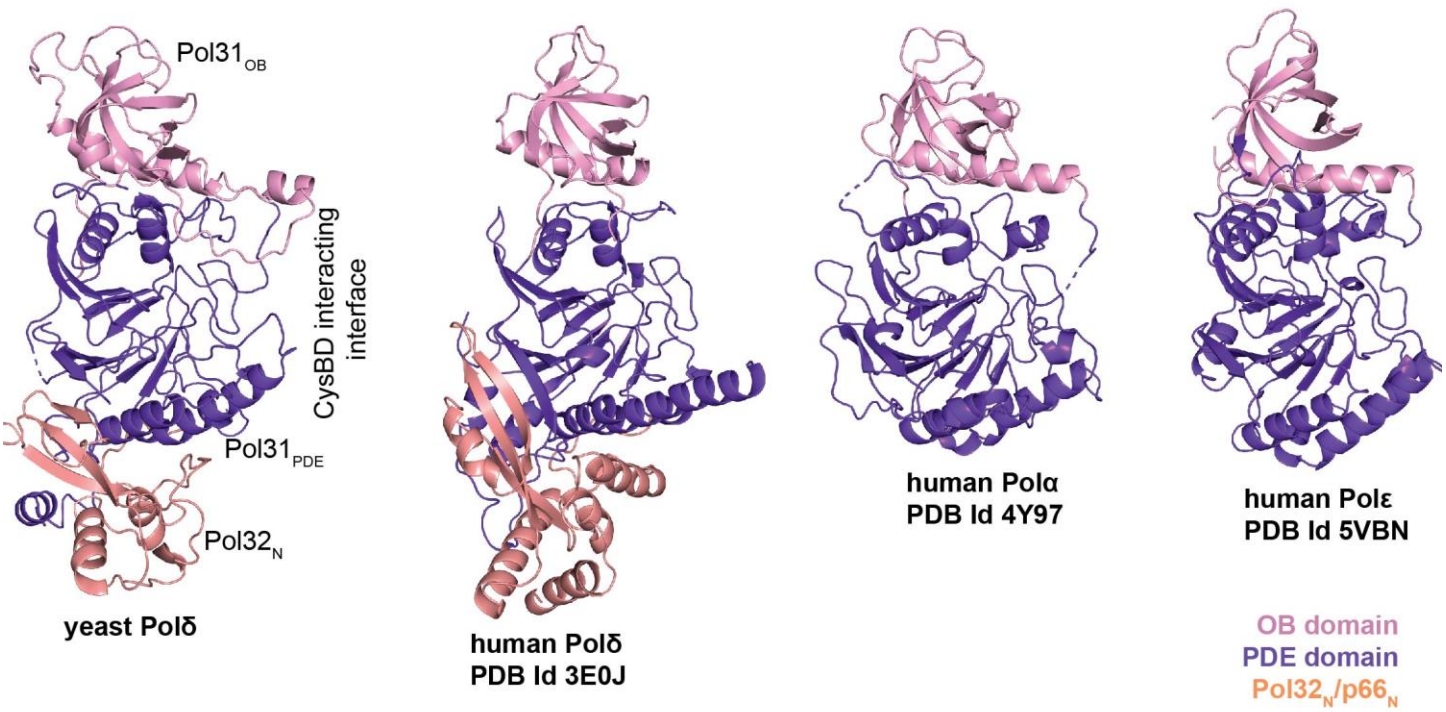

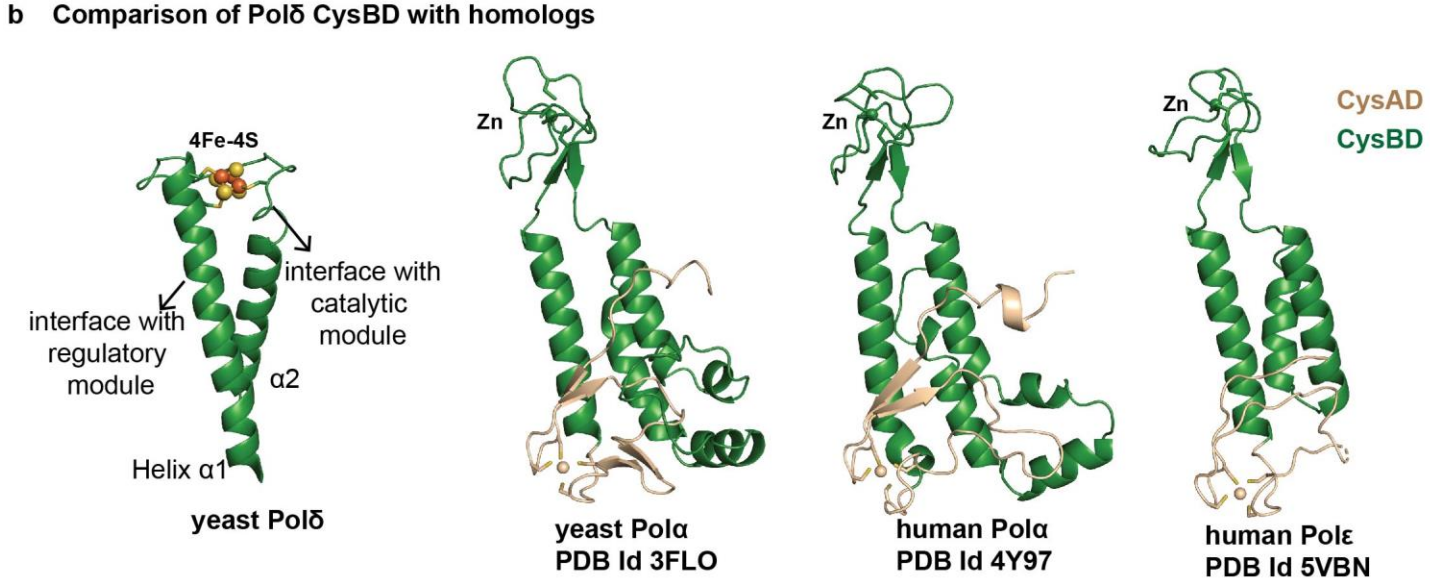

Supplementary Figure 2

Comparison of Polδ regulatory module and CysBD with those in homologs.

a: The CysBD interacting interface of the regulatory module is substantially different between yeast Polδ, human Polδ, human Polα, and human Polε**. b:** CysBD of yeast Polδ is much smaller in size than the counterparts from pols α and ε. CysAD is disordered in yeast Polδ.

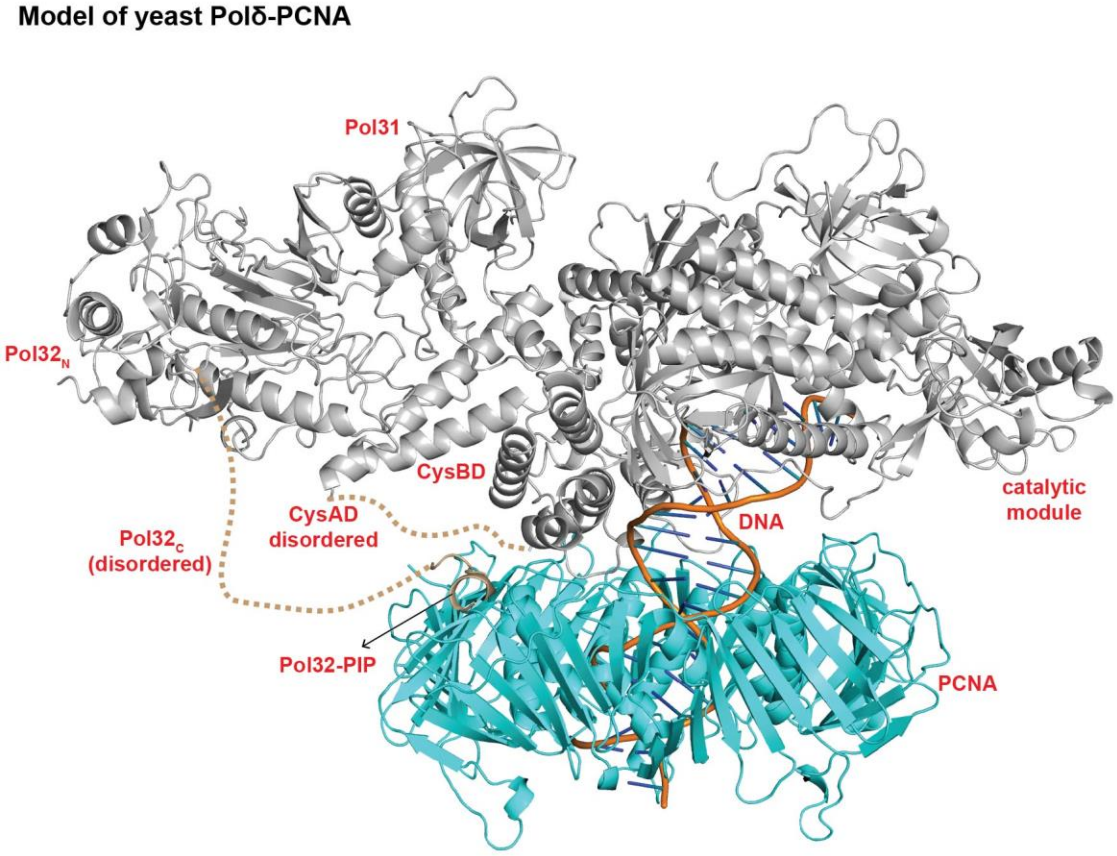

Supplementary Figure 3

Model of Polδ-PCNA complex.

Model of yeast Polδ (this work) and PCNA (PDB Id. 2OD8) derived by threading the Polδ bound DNA through the central hole of the PCNA.

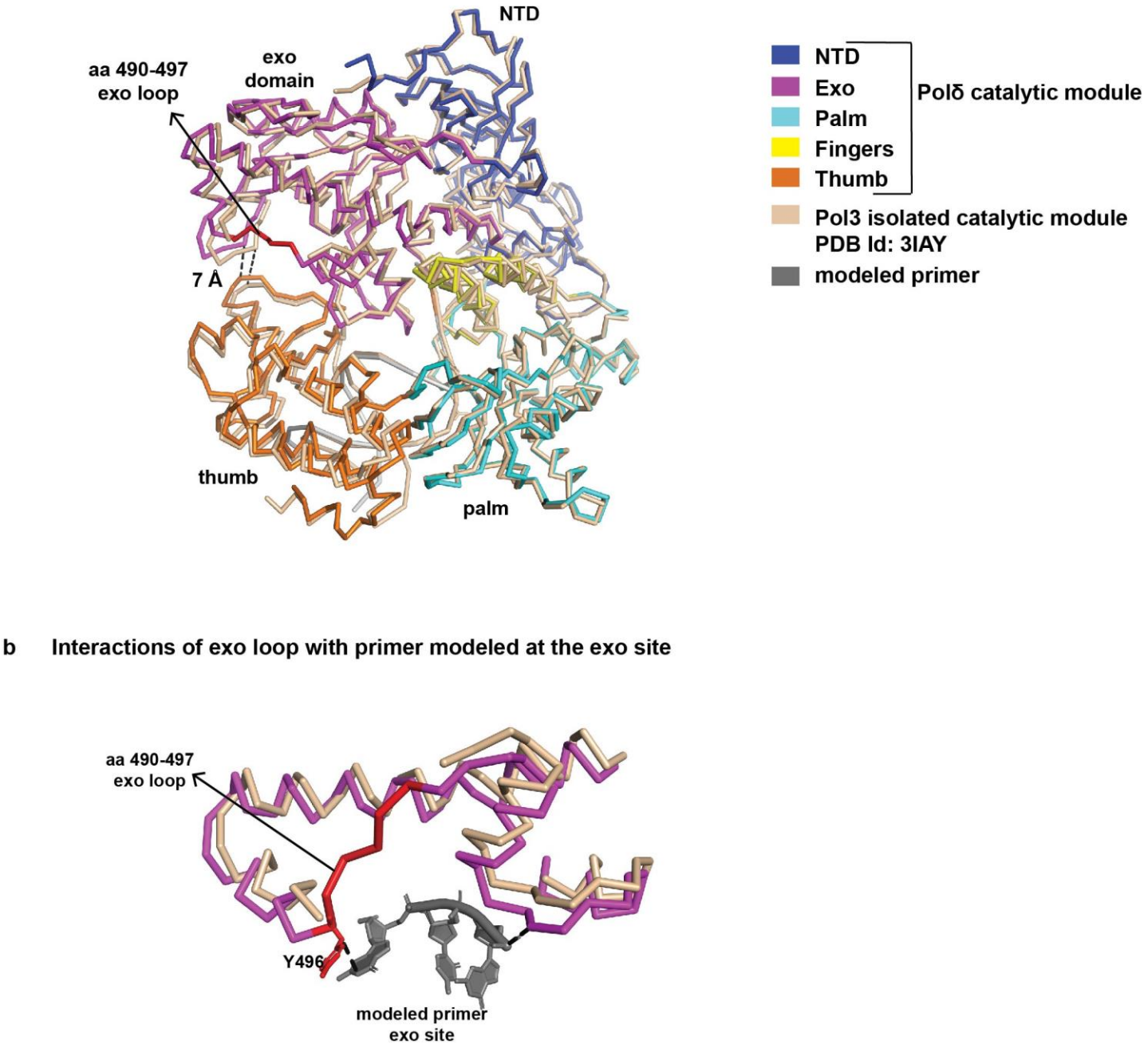

Supplementary Figure 4

CysBD mediated changes in the Pol3 catalytic module.

a: CysBD draws the exo and thumb domains of the catalytic module closer than their positions in the structure of the isolated catalytic module (3IAY) and results in an overall compaction of the catalytic module by > 2.5 Å **b:** A primer modeled at the exo active side is within van der Waals distance from Tyr496 which is part of the exo domain loop encompassing amino acids 490-497 that interacts with CysBD. This loop is disordered in the structure of the isolated catalytic module (3IAY).

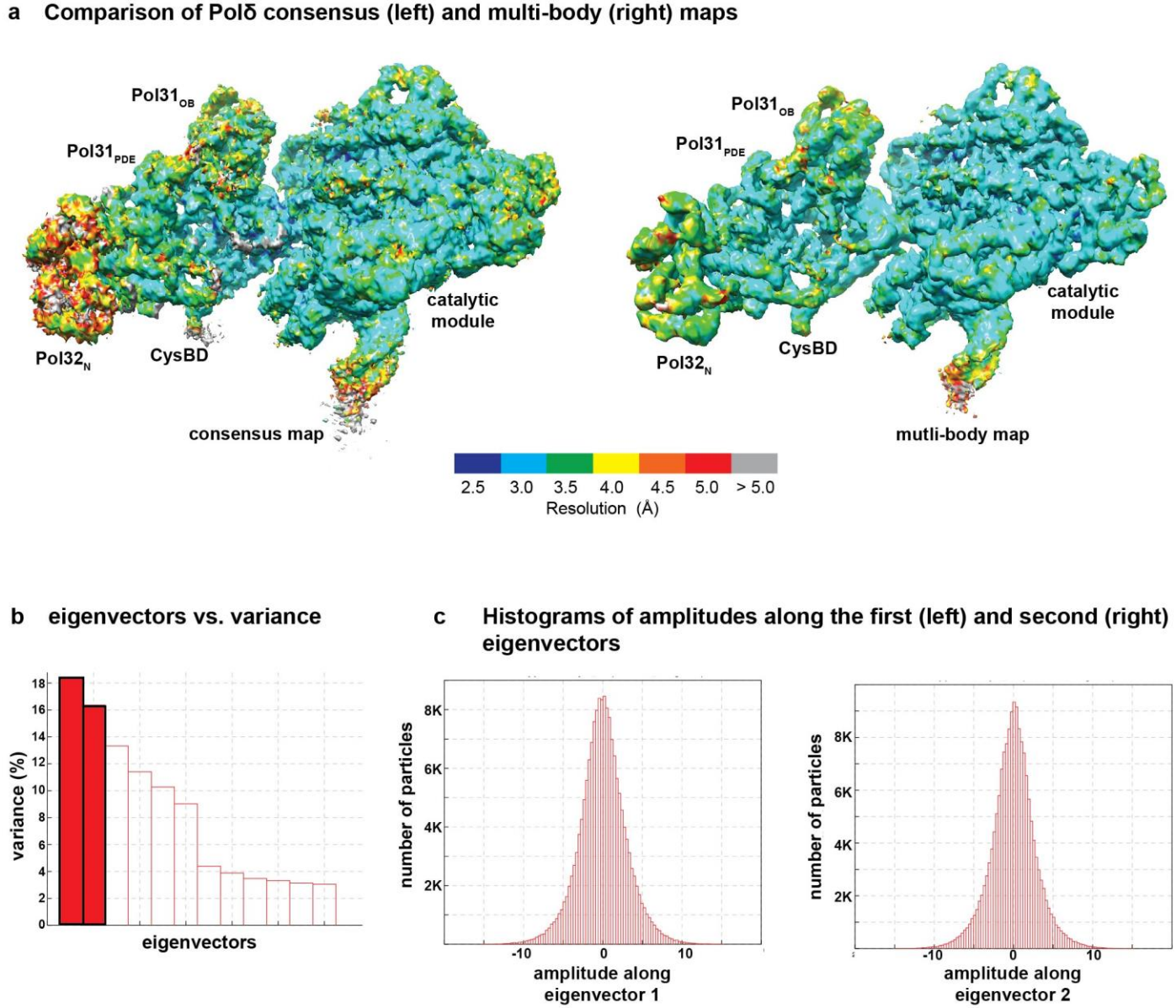

Supplementary Figure 5

Multi-body refinement and principal component analysis of the relative orientations of the catalytic and regulatory modules.

a: Consensus and multi-body maps colored by local resolution. Multi-body analysis results in a substantial improvement in resolution for regions of Pol31 and Pol32 that are farthest from the catalytic module, e.g. $Pol32_N$ and the OB fold of Pol31. **b:** Contribution of all eigenvectors to the variance. **c:** Histograms of amplitudes along the first two eigenvectors. Both histograms are unimodal, indicating continuous motion.

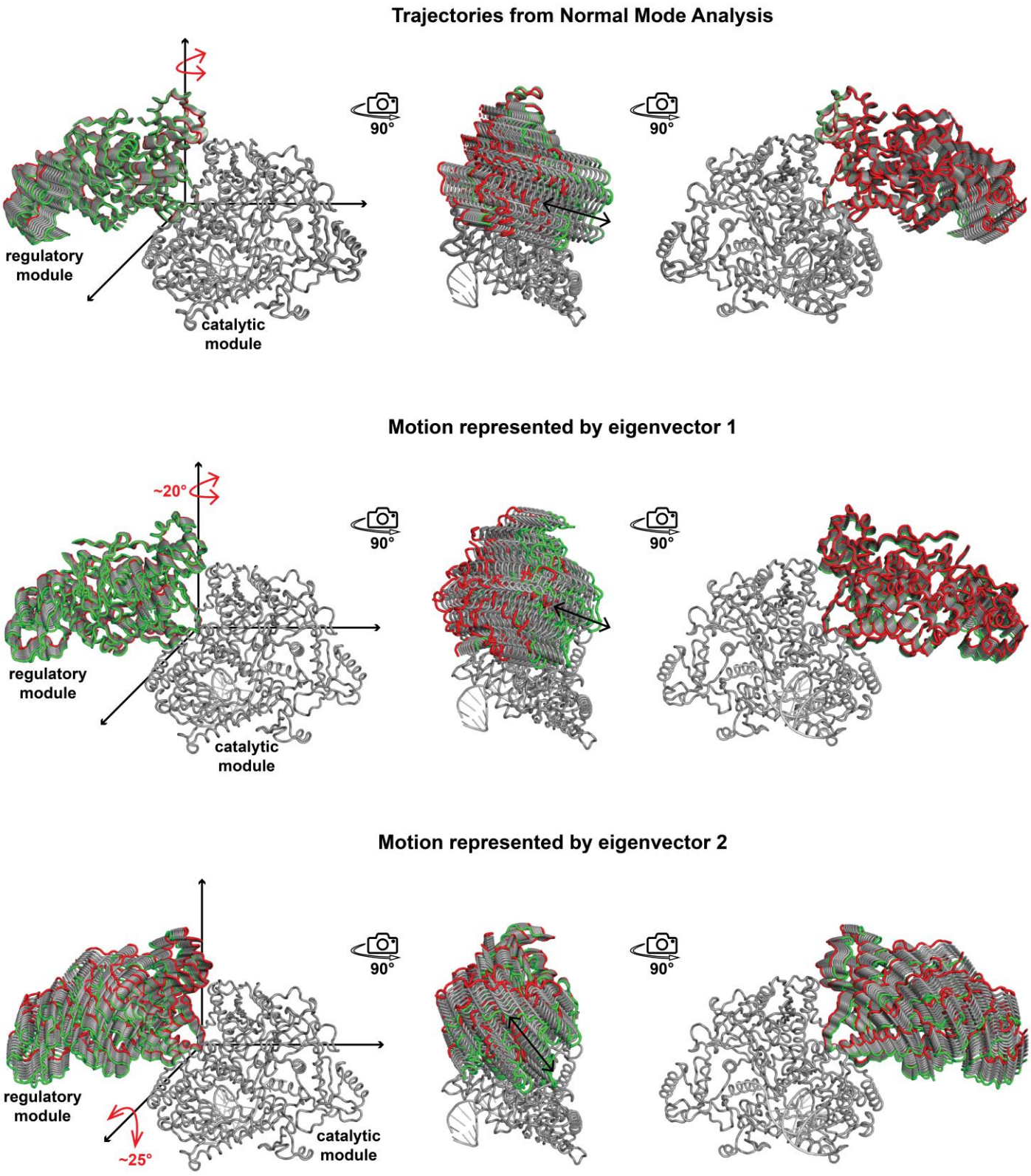

Supplementary Figure 6

Trajectories from normal mode analysis compared to motion from multi-body analysis.

End of range conformations for the regulatory module are shown in green and red. The first eigenvector from principal component analysis of multi-body refinement represents rocking motion of the regulatory module parallel to the catalytic module (middle), while the second eigenvector represents rocking motion towards the catalytic module (bottom). Trajectories for the first non-trivial mode of molecular motion from Normal Mode Analysis (top) corresponds to the motion represented by the first eigenvector (middle).

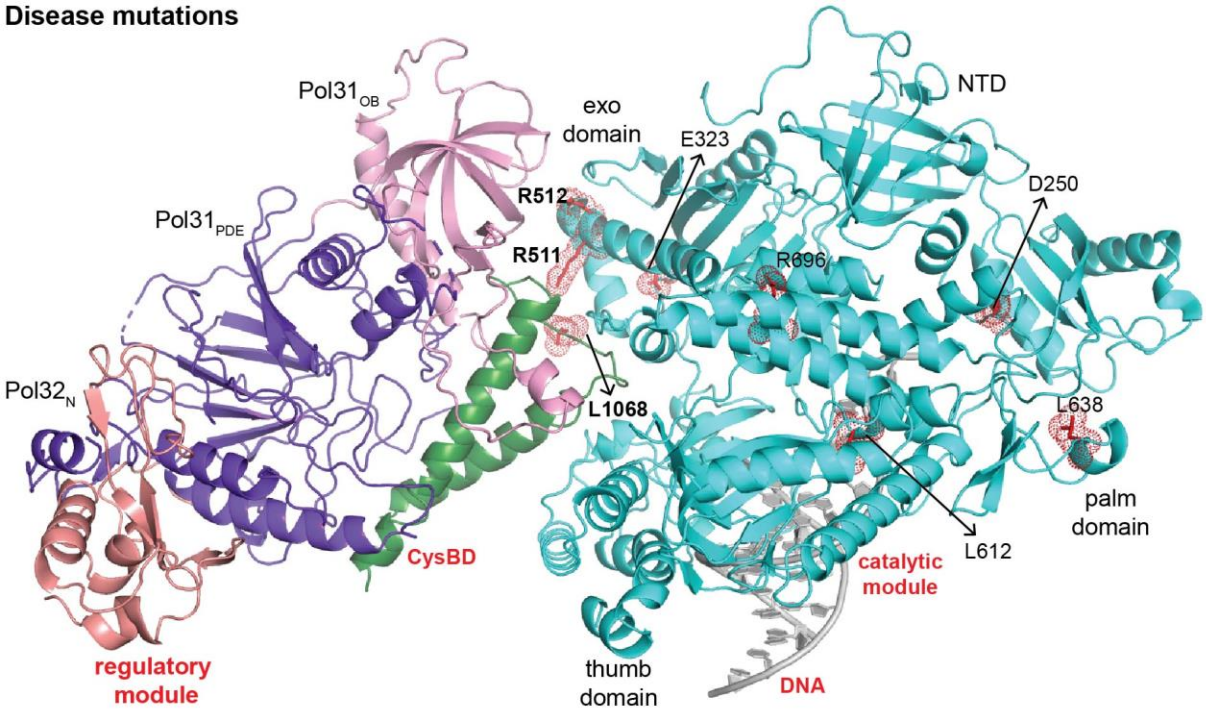

	human mutation	yeast equivalent	domain	disease	status
1	E245K	D250	NTD	cancer	driver
2	E318K	E323	exo	cancer	driver
3	L606M	L612	palm	cancer	driver
4	L632M	L638	palm	cancer	driver
5	R689W	R696	fingers	cancer	driver
6	R1016H	K1013	CysAD	cancer	driver
7	**R506H**	**R511**	**Exo / Interface**	**cancer**	**unknown status**
8	**R507C**	**R512**	**Exo / Interface**	**MDPL**	
9	**I1070N**	**L1068**	**CysBD / Interface**	**MDPL**	

Supplementary Figure 7

Disease mutations in human Polδ.

Cancer driver mutations in human Polδ mapped on the structure of yeast Polδ (top). These mutations are distributed on the NTD, exo, palm, fingers and CysAD domains. The oncogenic R506H (exo) mutation and the MDPL associated R507C (exo) and I1070N (CysBD) mutations map to the interface between the catalytic and regulatory modules.